

# Simulating continuous symmetry models with discrete ones

A. G. Catalano,<sup>1,2</sup> D. Brtan,<sup>3</sup> F. Franchini,<sup>1,\*</sup> and S. M. Giampaolo<sup>1,†</sup>

<sup>1</sup>*Institut Ruđer Bošković, Bijenička cesta 54, 10000 Zagreb, Croatia*

<sup>2</sup>*Université de Strasbourg, 4 Rue Blaise Pascal, 67081 Strasbourg, France*

<sup>3</sup>*SISSA and INFN, via Bonomea 265, 34136 Trieste, Italy*

It is known that frustrated systems display unusual properties. Even the seemingly weak contribution of topological frustration can bring an anisotropic Heisenberg chain, which is defined by discrete local symmetries, to develop characteristics that are usually associated to continuous symmetries and a gapless spectrum, such as a finite Fermi momentum. We show that, in a region of this model's phase diagram, an adiabatic change in the system's parameters causes a singular orthogonality catastrophe so that neighboring ground states are exactly orthogonal for any system size, due to a flow in the states' quantum numbers. The chain also acquires unusual features such as ground states with non-zero chirality and a breaking of invariance by translation. However, the amplitude of these attributes decay to zero in the thermodynamic limit. This region of parameter space (chiral region) is separated from the rest by a transition line where also any non-analyticity vanishes in the thermodynamic limit, even though the ground state degeneracy changes crossing this line. We pose that this line can constitute a boundary-BKT-like transition.

## I. INTRODUCTION

One-dimensional spin-1/2 systems have always represented an important field of study for the physics of quantum many-body systems, but nowadays their relevance is growing. Indeed, if for a long time they have represented toy models useful to detect features that can be embedded into frameworks of more realistic systems, in the last years, several newly developed experimental devices [1–4] have allowed for their realization, thus disclosing the path towards direct tests of the theoretical predictions. Assuming invariance under spatial translation and limiting to systems with finite range interactions, in agreement with Goldstone's theorem [5, 6], they are usually classified into two large families. The first includes models in which Hamiltonians show only discrete local symmetries that can be associated only with finite sets of quantum numbers, i.e. sets of distinct eigenvalues of operators commuting with the Hamiltonian. In the thermodynamic limit, these models are characterized by ordered phases in which systems hold degenerate ground-state manifolds, separated by finite energy gaps from the rest of the spectrum. These manifolds contain elements characterized by different quantum numbers and therefore, by combining them, it is possible to construct ground-states violating at least one of the Hamiltonian's symmetries. Such states can be characterized by non-zero order parameters, i.e. non-vanishing expectation values for operators that should otherwise vanish due to symmetry. On the other side, we have models showing also local continuous symmetries. These symmetries are characterized by sets of quantum numbers whose size scales with the chain length and that tend to a continuum in the thermodynamic limit. In these models properly ordered phases are

absent [7], although quasi-long-range-order can still exist in gapped phases. At criticality, the gap-less energy spectrum can be characterized by continuous cross-overs among symmetry preserving ground states with different quantum numbers.

Think, for instance, of an  $XXZ$  spin-1/2 chain, in which eigenstates can be classified by their (conserved) magnetization in the  $z$  direction, as a reflection of its continuous  $U(1)$  rotational symmetry. At zero external field, there is a finite interval in the  $z$ -anisotropy for which the model is gapless and the ground state has vanishing magnetization. Turning on an external magnetic field on the  $z$  axis can keep criticality, but now the lowest energy state acquires a finite magnetization [8]. As the external field changes, the system undergoes a series of crossings between states that, being characterized by different quantum numbers, are perfectly orthogonal to each other. Since, in the thermodynamic limit, the magnetization tends to a continuum, systems like this present an extreme case of orthogonality catastrophe [9, 10] in which any change in the Hamiltonian parameters adiabatically moves between states with zero overlap [11]. Another important quantity characterizing system like the  $XXZ$  chain is the existence of a *Fermi momentum*, identifying the momentum of low energy excitation.

The situation in models with discrete symmetries is usually very different, because no Fermi energy can be defined and each state can be characterized by a finite set of quantum numbers. However, as we will show in the present work, it is possible to mimic the peculiar behavior of models with continuous symmetries in the framework of systems with discrete ones. As we will see, in the latter case translational invariance becomes the relevant symmetry to classify states by, given that the number of Fourier modes scale with the system size. In particular, we will show that a system with discrete symmetries can present a continuous crossover between orthogonal ground states with different quantum numbers (lattice momenta), similar to that of critical phases in systems

\* fabio@irb.hr

† sgiampa@irb.hr

with a continuous symmetry.

With the help of both numerical diagonalization and analytical evaluations, we will demonstrate that such crossovers can be realized in short-range completely anisotropic  $XYZ$  chains with a local external field when a frustration [13–19] of topological origin is induced. Topological frustration arises when, in a short-range antiferromagnetic system made of an odd number of spins, periodic boundary conditions are imposed, thus realizing the so-called frustrated boundary conditions (FBC) [12, 20–23]. We will show that these models present a region of parameter space, which we name the *chiral region*, in which even at finite sizes several two-fold degenerate manifolds play, alternatively, the role of ground states. Such manifolds, whose elements have the same parity in their magnetization, are spanned by two eigenstates with opposite quantum numbers for the momentum operator. Increasing the size of the system, the possible values of the momentum quantum number grow, hence increasing also the number of crossovers in the chiral region. Thereby, in the thermodynamic limit, it will show a behavior mimicking the critical phase of models with local continuous symmetry. Moreover, these ground state momenta act as Fermi points and low energy excitations lie close to them. The chiral region is separated from the rest of the parameter space by a BKT-boundary like transition in which the degeneracy of the ground state changes but none of the derivatives of the energy show non-analytic behavior. Consistently with the fact that this transition is induced by the particular choice of boundary conditions, all the parameters we have analyzed in the attempt to classify the chiral region vanish algebraically with the chain length.

To better characterize this region, we focus our attention to the ground-state fidelity [24–27, 29–31]. Given a parametric Hamiltonian  $H(\vec{\lambda})$ , the ground-state fidelity is the overlap between the ground states corresponding to two slightly different sets of parameters  $\vec{\lambda}$  and  $\vec{\lambda} + d\vec{\lambda}$ . In a system with discrete symmetries, the ground state changes smoothly, and hence the ground-state fidelity per site is expected to be very close to 1 except close to a quantum critical point. There, the rearrangement of the macroscopic properties induces its sudden drop, which is mirrored by the behavior of the fidelity susceptibility. On the other hand, in the gapless phase of systems with local continuous symmetries, each point is characterized by a crossover between two states with different quantum numbers that are orthogonal to each other, and hence the fidelity is identically zero. In our case, the ground-state fidelity shows behavior that falls in between these two cases. While moving along almost every direction in the parameter space, the system changes the ground-state momentum, making the fidelity drop to zero. But there exists a particular direction along which the momentum stays constant and the fidelity shows a more regular behavior. The same behavior is observed, for instance, in the  $XXZ$  chain discussed above: changing the interaction strength while keeping the external field fixed allows

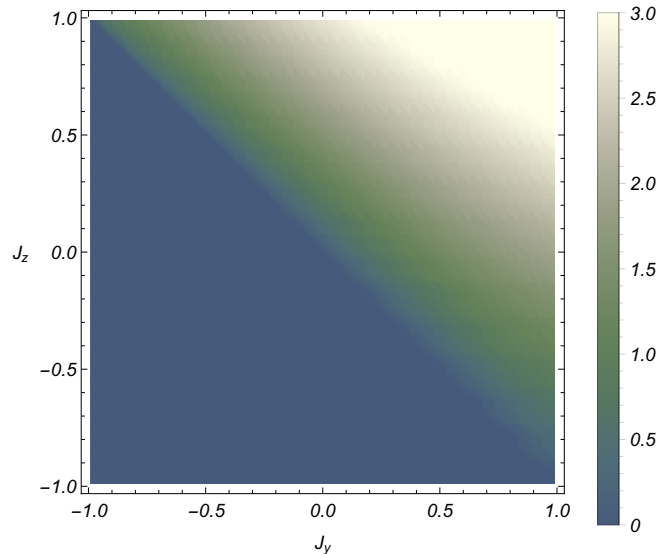


FIG. 1: Dependence of the threshold value  $h^*$  as a function of  $J_y \in (-1, 1)$  and  $J_z \in (-1, 1)$  for  $N = 15$  and  $J_x = 1$ . For  $|h| < h^*$  (the *chiral region*) the ground state manifold is at least two-fold degenerate and spanned by states with finite and opposite momentum.

for the fidelity to have a regular behavior. We present a complete analysis of the geometrical property of the ground state based on the fidelity through a reduced density matrix, following the path suggested in [11] and show that this quantity scales differently between models with discrete and continuous symmetry.

The paper is organized as follows. In the second section, we present several numerical results, obtained with an exact diagonalization approach, that depicts the main features of the chiral region. In the third section, to analyze how these features scale towards the thermodynamic limit, we restrict to the  $XY$  model in which we can exploit the fact that the model can be exactly mapped to a free-fermionic system and hence can be solved analytically. Due to this fact, we show that both the violation of the invariance under spatial translation and the chirality vanish in the thermodynamic limit and that, at the boundary of the chiral region, none of the energy derivatives show non-analyticities. To better characterize this peculiar region, in the fourth chapter we study both the total ground-state fidelity, which drops to zero in the continuous-symmetry-like region, and the reduced one. In the end, we present our conclusions.

## II. ANISOTROPIC XYZ CHAIN

We focus on the generic short-range completely anisotropic Heisenberg model in the presence of a local field directed along with one of the spin directions that, without losing generality, we assume to coincide with the

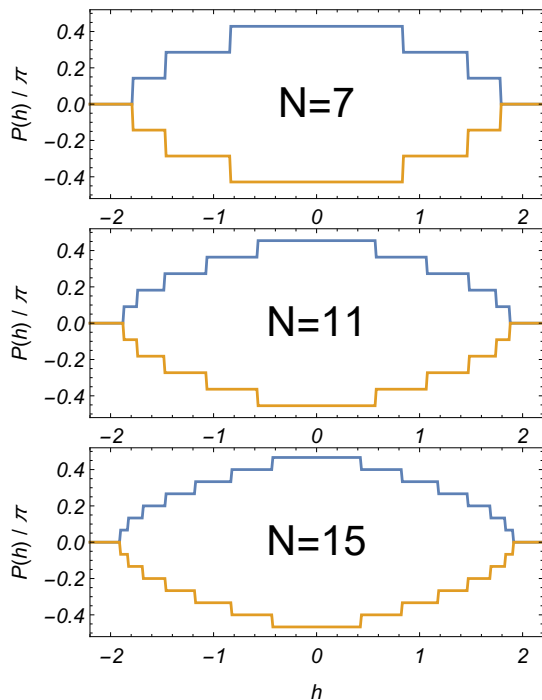


FIG. 2: Ground-state momenta  $p(h)$  in unit of  $\pi$  as function of the local field amplitude  $h$  for different sizes of the chain at fixed values of the anisotropies (note that momenta are compactified between  $-\pi/2$  and  $\pi/2$ ). The data are obtained setting  $J_x = 1.0$ ,  $J_y = 0.6$  and  $J_z = 0.2$ . Note that, except in the cases of a zero ground state momentum, the ground state manifold is always twofold degenerate with the two ground states carrying opposite momenta. Moving in phase space, the ground state vectors acquire all momenta allowed by the quantization rules.

$z$  axis. To induce a frustration of topological origin, we restrict our analysis to the case of a system made of an odd number of spins with periodic boundary conditions in which the dominant interaction is antiferromagnetic. The Hamiltonian of such a system reads

$$H = \sum_{j=1}^N \sum_{\alpha=x,y,z} J_{\alpha} \sigma_j^{\alpha} \sigma_{j+1}^{\alpha} - h \sum_{j=1}^N \sigma_j^z, \quad (1)$$

where  $\sigma_j^{\alpha}$ , for  $\alpha = x, y, z$ , are Pauli matrices and the periodic boundary conditions require  $\sigma_j^{\alpha} = \sigma_{j+N}^{\alpha}$ . The couplings  $J_{\alpha}$  fix the strength of the interactions and we assume that  $J_x \neq J_y$  to avoid the system acquiring a higher symmetry of invariance under the rotation by any angle around the  $z$  axis. As a consequence, the system holds only the discrete parity symmetry along  $z$  ( $\Pi^z = \prod_{i=1}^N \sigma_i^z$ ) that, independently on the system size, admits only two quantum numbers ( $\pm 1$ ).

Using an in-house code based on the Lanczos algorithm, we numerically solve the Hamiltonian in eq. (1) for several odd  $N$ . Keeping  $J_x = 1$  and assuming  $J_x >$

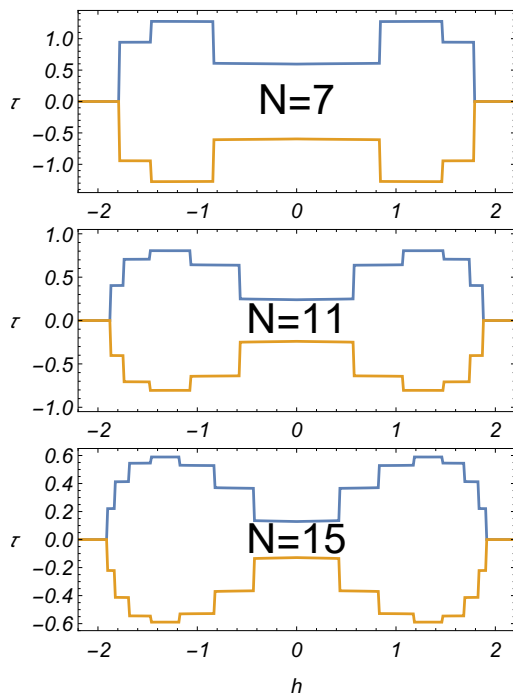


FIG. 3: Ground-state chirality  $\tau$ , evaluated on the elements of the ground-state manifolds that are also eigenstates of the lattice momentum operator, as a function of the local field amplitude  $h$  for different sizes of the chain at fixed values of the anisotropies. A finite chirality reflects the finite momentum carried by the ground state vector, indicating that in its lowest energy state, the system moves in a stationary way. The data are obtained settings  $J_x = 1.0$ ,  $J_y = 0.6$  and  $J_z = 0.2$ .

$|J_y|, |J_z|$ , we obtain that in the region  $J_z > -J_y$  there is a threshold value of the local field  $h^* > 0$ , which delimits the chiral region, such that for each  $h \in (-h^*, h^*)$  the ground-state manifold is at least two-fold degenerate (see Fig. 1). Such a manifold is completely described by the states  $|\pm p\rangle$  with opposite values of the momentum quantum number  $\pm p(h)$ , as it can be seen in Fig. 2. This momentum  $p(h)$  acts as a Fermi point, in a system whose discrete symmetry should not allow for its existence, as low energy excitations must lie nearby. Moving  $h$  throughout the region  $(-h^*, h^*)$ , the system visits all possible values of the momentum quantum number. Since states with different quantum numbers are orthogonal to each other and the size of the set of the momentum quantum numbers scales with the chain length, the number of different crossovers occurring in the region  $(-h^*, h^*)$  increases with  $N$ .

It is worth noting that, differently from what usually happens in the ordered phase of the models showing only discrete local symmetries, this degeneracy in the ground-state manifold is present even at finite sizes and involves states in the same sector of the parity  $\Pi^z$ . Such degeneracy stems from mirror symmetry with re-

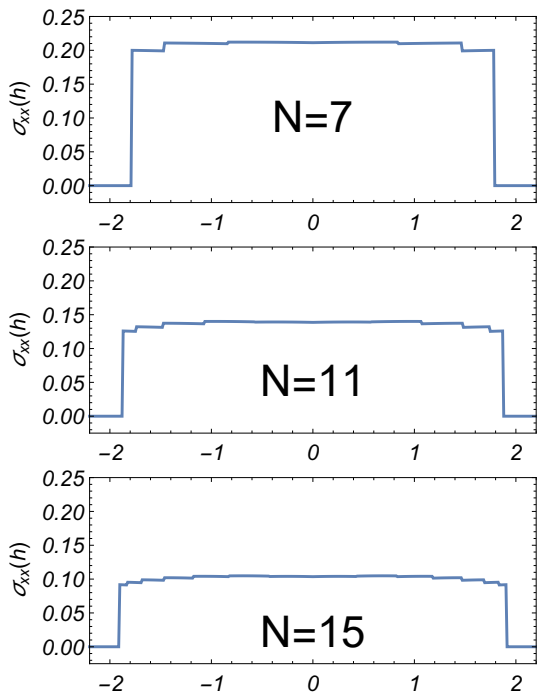


FIG. 4: Variance  $\sigma_{xx}(h)$  of expectation values of  $\sigma_i^x \sigma_{i+1}^x$ , which varies in space, as function of the external field  $h$  for  $J_x = 1.0$ ,  $J_y = 0.6$  and  $J_z = 0.2$ . The data are obtained using the ground state vector  $\frac{1}{\sqrt{2}}(|p\rangle + |-p\rangle)$ . The variance is finite for  $|h| < h^*$ , although decreasing with the chain length, indicating that indeed the two point function is not translational invariant.

spect to any site, which implies that each eigenstate has to be at least two-fold degenerate, with the only exception of zero momentum states [12]. This peculiar structure of the ground-state manifold has some interesting implications. The first is that, since in the chiral region  $(-h^*, h^*)$  the ground-states typically have a non-vanishing momentum, they are expected to be characterized by a non-zero expectation value of the chiral operator  $\hat{\tau} \equiv \vec{\sigma}_{i-1} \cdot \vec{\sigma}_i \wedge \vec{\sigma}_{i+1}$  [32, 33]. To show this fact, in Fig. 3 we plot the behavior of the site independent expectation value  $\tau \equiv \langle \pm p | \hat{\tau} | \pm p \rangle$ . On the other side, a ground state that is a linear superposition of  $|\pm p\rangle$ , violates the invariance under spatial translation of the Hamiltonian. This fact can be highlighted by analyzing the variance of the spatial distribution of the two-body next-neighbor spin correlation function along  $x$ , i.e. the expectation values of  $\sigma_i^x \sigma_{i+1}^x$ , on the state  $\frac{1}{\sqrt{2}}(|p\rangle + |-p\rangle)$ . Fixing  $J_x = 1$ ,  $J_y = 0.6$  and  $J_z = 0.2$  the variances as a function of the local field obtained with the exact diagonalization approach are depicted in Fig. 4.

### III. XY MODEL

In the previous section, we presented the main characteristics of the chiral region, where the ground state vectors acquire a finite momentum and a system with discrete symmetries mimics the behavior of a system with continuous symmetries. However, to study how these properties scale with the system size, we need to consider chains much longer than those accessible within an exact diagonalization approach. Even advanced numerical methods, such as DMRG are not easily applicable to models showing topological frustration, especially in the region of interest of the present work, due to the simultaneous degeneracy between ground-states in the same parity sector and the closing of the energy gap between the ground-states and the immediately overlying excited states in the thermodynamic limit.

Therefore, to push our study towards larger sizes we now focus on the case  $J_z = 0$  which can be mapped to a free-fermionic model, thus disclosing the possibility for an analytical solution. Introducing the anisotropic parameter  $\gamma$  and defining  $J_x = \frac{1+\gamma}{2}$  and  $J_y = \frac{1-\gamma}{2}$ , the Hamiltonian of the model in (1) reduces to the one of the XY model in a perpendicular field

$$H = \sum_{j=1}^N \left[ \frac{1+\gamma}{2} \sigma_j^x \sigma_{j+1}^x + \frac{1-\gamma}{2} \sigma_j^y \sigma_{j+1}^y - h \sigma_j^z \right]. \quad (2)$$

For the sake of simplicity, we limit our analysis to the case with  $h \geq 0$  and  $0 < \gamma \leq 1$ , but our results can be easily extended also to the other regions of the parameters space. As it is well-known, the Hamiltonian in (2) can be solved using a standard approach, which consists of a Jordan-Wigner transformation that maps the spin degrees of freedom into spinless fermions, followed by a Fourier and a Bogoliubov transformation which completes the diagonalization in the space of the lattice momenta [8]. A detailed analysis of this approach in presence of FBC along with the derivation of the ground-states and their properties can be found in the appendix. In the end, these operations reduce the Hamiltonian to the form

$$H = \frac{1 + \Pi^z}{2} H^+ + \frac{1 - \Pi^z}{2} H^- + \frac{1 - \Pi^z}{2} H^- - \frac{1 - \Pi^z}{2} H^-, \quad (3)$$

where  $H^\pm$  are given by

$$H^- = \sum_{q \in \Gamma^- / \{0\}} \Lambda(q) \left( b_q^\dagger b_q - \frac{1}{2} \right) + \epsilon(0) \left( b_0^\dagger b_0 - \frac{1}{2} \right) \quad (4a)$$

$$H^+ = \sum_{q \in \Gamma^+ / \{\pi\}} \Lambda(q) \left( b_q^\dagger b_q - \frac{1}{2} \right) + \epsilon(\pi) \left( b_\pi^\dagger b_\pi - \frac{1}{2} \right), \quad (4b)$$

Here  $b_q$  ( $b_q^\dagger$ ) are the Bogoliubov annihilation (creation) fermionic operators with the lattice momenta  $q$  that, due to the quantization conditions, belong to two different sets  $\Gamma^- = \{\frac{2\pi n}{N}\}_{n=0}^{N-1}$  for the odd  $\Pi^z$  sector and  $\Gamma^+ =$

$\{\frac{2\pi}{N}(n+\frac{1}{2})\}_{n=0}^{N-1}$  for the even one. The dispersion relation  $\Lambda(q)$  for  $q \neq 0, \pi$  obeys

$$\Lambda(q) = \sqrt{(h + \cos q)^2 + \gamma^2 \sin^2 q}, \quad (5)$$

while for the two specific modes  $q = 0 \in \Gamma^-$  and  $q = \pi \in \Gamma^+$  we have

$$\epsilon(0) = h + 1, \quad \epsilon(\pi) = h - 1. \quad (6)$$

It is important to observe that, having assumed  $h > 0$ , all fermionic modes in the odd sector are associated with a positive energy, while in the even sector there is also a (single) negative contribution to the total energy coming from a fermion with momentum  $q = \pi$  if  $h < 1$ .

The knowledge of the energy contribution of every single fermionic mode allows to explain how and when the continuous-symmetry-system-like behavior rises. Indeed, for  $h < h^* \equiv 1 - \gamma^2$ , the dispersion relation in (5) develops two symmetric minima at  $q = \pm \tilde{q}$  with

$$\tilde{q} = \arccos\left(\frac{h}{\gamma^2 - 1}\right). \quad (7)$$

Note that the threshold parabola  $h = 1 - \gamma^2$  differs from the usual circle  $h^2 + \gamma^2 = 1$  that encloses the region with oscillatory contributions to the correlation functions in the non-frustrated XY chain.

In general, for finite size systems,  $\tilde{q}$  is not an allowed lattice momentum of the system. Therefore let us define  $\tilde{q}^+$  and  $\tilde{q}^-$  as the momenta in the even and in the odd sectors closest to  $\tilde{q}$ . Since in the odd parity sector, there is no fermionic mode with a negative energy contribution, the lowest energy is associated to the states  $|\pm \tilde{q}^-\rangle = b_{\pm \tilde{q}^-}^\dagger |\emptyset^-\rangle$  where  $|\emptyset^-\rangle$  stands for the fermionic vacuum state in the odd parity sector. On the contrary, in the even parity sector, since  $h < 1$ , the mode with momentum  $\pi$  has negative energy. However, because of the parity constraint, we cannot populate only the  $\pi$  mode. That is why the lowest energy state is the vacuum, as no fermionic mode has energy lower (in absolute value) than that of the  $\pi$  mode. However, for  $h < h^*$  the minima energy of the  $\pm \tilde{q}^+$  modes is smaller than  $1 - h$ . Thus, because the net contribution of the these two modes provides a negative energy,

the two lowest energy states in the even sector are  $|\pm \tilde{q}^+\rangle = b_{\pm \tilde{q}^+}^\dagger b_\pi^\dagger |\emptyset^+\rangle$ , where  $|\emptyset^+\rangle$  stands for the fermionic vacuum state in the even parity sector. It is worth noting that, even if both  $|\emptyset^+\rangle$  and  $|\emptyset^-\rangle$  describe fermionic vacuum states, they are defined on different modes, and hence they are separate states. The four states, i.e.  $|\pm \tilde{q}^+\rangle$  and  $|\pm \tilde{q}^-\rangle$  have a lattice momentum respectively equal to  $\pm(\pi + \tilde{q}^+)$  and  $\pm \tilde{q}^-$  [12] and their associated

energies are:

$$\begin{aligned} E_e &= \langle \pm \tilde{q}^+ | H | \pm \tilde{q}^+ \rangle \\ &= \Lambda(\tilde{q}^+) + \frac{\epsilon(\pi)}{2} - \frac{1}{2} \sum_{q \in \Gamma^+ / \{\pi\}} \Lambda(q); \end{aligned} \quad (8a)$$

$$\begin{aligned} E_o &= \langle \pm \tilde{q}^- | H | \pm \tilde{q}^- \rangle \\ &= \Lambda(\tilde{q}^-) - \frac{\epsilon(0)}{2} - \frac{1}{2} \sum_{q \in \Gamma^- / \{0\}} \Lambda(q). \end{aligned} \quad (8b)$$

In each sector, the lowest energy state is separated from the other eigenstates by a gap that closes like  $1/N^2$ , with the lightest states having finite momenta close to  $\tilde{q}$ , as can be easily understood from the dispersion relation in eq. (5). Thus,  $\tilde{q}^\pm$  act as an effective Fermi momentum and one can think of the states spanning each ground state manifold as resulting from a shell-filling effect that keeps only one of the two Fermi points occupied.

To better understand the ground state structure, let us start with the assumption that we choose the parameters of the Hamiltonian such that  $\tilde{q}$  coincides with  $\tilde{q}^+$ . Thus, the ground-state manifold is spanned by the states  $|\pm \tilde{q}^+\rangle$  and belongs to the even parity sector. A generic change in the parameters  $h$  and  $\gamma$  will move  $\tilde{q}$  away from  $\tilde{q}^+$  and bring it progressively closer to  $\tilde{q}^-$ . At some point  $E_o$  becomes smaller than  $E_e$  and there will be a crossover between the states  $|\pm \tilde{q}^+\rangle$  and  $|\pm \tilde{q}^-\rangle$ , with the ground-state manifold switching to the odd parity sector. Further moving the parameters in the same direction, eventually  $\tilde{q}$  will come close to a different allowed momentum in the even sector. Hence the system will face a second crossover, and this process will continue until the parameters of the Hamiltonian exit from the chiral region  $|h| < h^*$  and settle into the even parity fermionic vacuum as the ground state. Increasing the dimension of the system, the distance between the different momenta becomes progressively smaller and hence the crossing become denser until each point in the region will be characterized by a crossover between two two-fold degenerate manifold belonging to two different parity sectors and having different quantum numbers of the lattice momentum.

In this portrayal, we have assumed that changes in the system parameters always change  $\tilde{q}$ . However, from eq. (7), we see that we can keep the minimum of the dispersion relation fixed by moving along the parabola  $h = c(1 - \gamma^2)$ , where  $c$  is a constant defined in the interval  $[0, 1]$ . In chains of finite length, one can identify a strip around each parabola in which the ground state manifold remains constant and this strip becomes narrower as the chain length increases. In this way the system undergoes a foliation of the ground state space that is made of as many manifolds as is the number of sites in the system and which, therefore, diverges in the thermodynamic limit. Let us stress once more that, any time a change of parameters changes  $\tilde{q}^\pm$ , hence crossing a strip, even for small systems the fidelity suddenly drops to zero, thus representing an extreme instance of orthogonality catas-

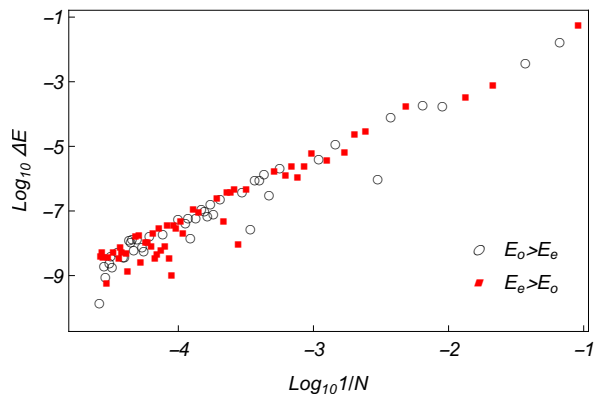


FIG. 5: Behavior of  $\Delta E = |E_e - E_0|$ , for  $h = 0.4$  and  $\gamma = 0.6$  as function of the system length  $N$ . The red squares represent points in which the states in the even sector have energy greater than the ones in the odd sector, while the black circle signals the presence of a ground state manifold living in the even sector. The parity of the ground state manifold keeps alternating as more sites are added.

trophe [9, 10].

At this point, the question that naturally arises is whether the chiral region represents a different thermodynamic phase or not. On one side, although the gap between the ground state and the first excited state closes proportionally to  $1/N^2$  in the whole frustrated phase for  $|h| < 1$ , for  $h^* < h < 1$  the ground state is always represented by the fermionic vacuum state  $|\emptyset^+\rangle$ , while in the chiral region the ground state manifold keeps changing its parity and momenta. Even increasing the chain length without moving  $h$  and  $\gamma$  can switch the ground state parity (see Fig. 5). Moreover, as can be appreciated from Fig. 5, the gap between the alternating ground states closes exponentially with the chain length, which means that in the thermodynamic limit the two manifold become effectively degenerate: crossing the line  $h = h^*$  the ground state degeneracy thus grows from 1 to 4, which could indicate a first order quantum phase transition.

However, analyzing the free energy derivatives (which at zero temperature coincide with the ground state energy) we cannot detect any discontinuity that remains finite in the thermodynamic limit. For  $h > h^*$  the ground state energy associated with the fermionic vacuum  $|\emptyset^+\rangle$  is

$$E_\emptyset = \langle \emptyset^+ | H | \emptyset^+ \rangle = -\frac{\epsilon(\pi)}{2} - \frac{1}{2} \sum_{q \in \Gamma^+ / \{\pi\}} \Lambda(q). \quad (9)$$

Immediately crossing into the chiral region, the ground state energy is the odd state one in eq. (8b) with  $\tilde{q}^- = \pi(1 - \frac{1}{N})$ . Starting from these two expressions for the energy below and above  $h = h^*$  it is possible to study the behavior of the derivatives at any order at the two sides of this line. Selecting a curve in the  $(h, \gamma)$  space, parametrized by a parameter  $\alpha$ , which crosses the  $h = h^*$

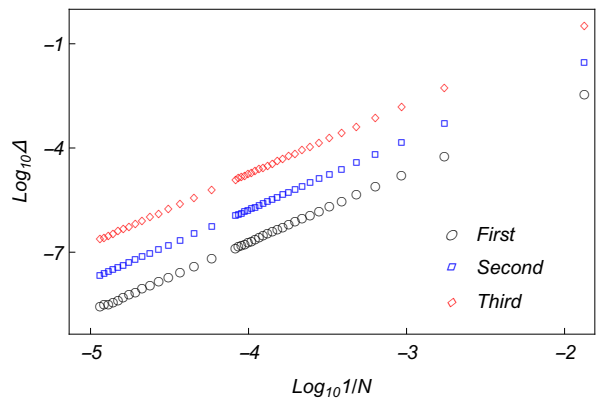


FIG. 6: Behavior of the jump in the energy derivatives  $\Delta(n)$ , for  $n = 1, 2, 3$  as a function of the inverse chain length, in logarithmic scale, obtained crossing the threshold  $h = h^*$  along a line with constant  $\gamma$ . The data are obtained setting  $\gamma = 0.6$ . All derivatives display a vanishing discontinuity in the thermodynamic limit.

curve at  $\alpha = 0$ , we compute

$$\Delta(n) = \left. \frac{\partial^n E_o}{\partial \alpha^n} \right|_{\tilde{q}^- = \pi(1-1/N)} - \frac{\partial^n E_\emptyset}{\partial \alpha^n}, \quad (10)$$

which must be finite, in the thermodynamic limit, to signal a traditional phase transition.

In Fig. 6 we show an instance of the dependence of  $\Delta(n)$  for  $n$  running from 1 to 3 when we cross the line  $h = h^*$  keeping  $\gamma$  fixed. As we can see below and above  $h^*$ , in the case of finite size systems, all the derivatives show a non-zero  $\Delta(n)$ , but these differences vanish proportionally to  $1/N^2$ . This fact implies that in the thermodynamic limit all the derivatives are analytical and hence that if  $h = h^*$  represents a quantum phase transition, it has to be one akin to a BKT transition [28].

This result is in stark contrast with the other phase transition induced by topological frustration discovered in models without external field [12]. In fact, in that transition, the first derivative of the ground-state energy shows a discontinuity that stays finite even in the thermodynamic limit. The reason behind this different behavior is that the transition point in Ref. [12] possesses a higher symmetry that produces a massive (thermodynamically large) ground state degeneracy. In this way, crossing this point, there is a true discontinuity and, for instance, the mode occupied in the odd parity sector of the ground state has momentum close to  $\pm \frac{\pi}{2}$ , instead of  $\pm \pi$  as we have here.

On the other hand, phase transitions are associated with a macroscopic reordering of the system properties that can be detected by opportunely chosen quantities. From what we have seen in the previous section, among others, two possible quantities can be considered: the chirality parameter that can detect the existence of ground-states with a non-vanishing momentum and the spatial variance of local observables that can highlight the vio-

lation of the invariance under spatial translation. Both these two quantities, and in general each spin correlation function on a ground-state with a fixed parity, can be obtained analytically in the framework of the analytical approach that we are using. The key point is the introduction of two different sets of Majorana operators so that each operator of a spin correlation function can be mapped to a string of Majorana ones. Hence, exploiting Wick's theorem the associated spin correlation functions can be reduced to the evaluation of a Pfaffian whose elements are the expectation values of two Majorana operators. As we show in the appendix, for  $h > h^*$  these expectation values can be classified in two different families: a) when the two Majorana operators come from the same set, the expectation value vanishes unless the two operators coincide; b) when the two Majorana operators come from different sets, the expectation value assumes values in the range  $[-1, 1]$  and are invariant under spatial translation. Entering the region  $h < h^*$  both these properties are changed. Indeed, the expectation values of Majorana operators coming from the same set but defined on different fermionic sites assume values proportional to  $1/N$  that hold the property to be invariant under spatial translation. On the other hand, the expectation values for Majorana in different sets acquire corrections proportional to  $1/N$  that explicitly violate the invariance under spatial translation.

These two corrections and their proportionality to  $1/N$  explain why both the chirality and the variance of the distribution of local quantities are different from zero in a finite frustrated system but disappear when the thermodynamic limit is taken into account. Indeed, using Wick's theorem, the expectation value of the chirality operator  $\tau$  can be reduced to a sum of products of expectations of pairs of Majorana fermions, with the peculiarity that each term in the sum contains at least an expectation on pairs of Majorana belonging to the same set, thus providing an algebraic decay with the system size to the whole expression. On the other hand, since all the site-dependent contributions to a local quantity scale with  $1/N$ , the variance is also vanishing in the thermodynamic limit. Both these behaviors should be compared to other observables calculated in presence of topological frustration in [12, 23]: there the  $1/N$  corrections coming from frustration appeared in combination with finite terms present also in absence of frustration and when an expectation value involved a sufficiently high number of corrections (also scaling with  $N$ ), the resulting expression brought finite contributions. The analytic derivation of both quantities can be found in the Appendix while in Fig. 7 and Fig 8 their dependence on the chain length is depicted for some relevant ground-states choice. The disappearance in the thermodynamic limit of both properties that characterize this region of the parameter space, associated with the absence of any local discontinuity in the energy derivatives on the line  $h = h^*$  support the idea that we are looking at a boundary transition whose effects disappear when the size of the system diverges.

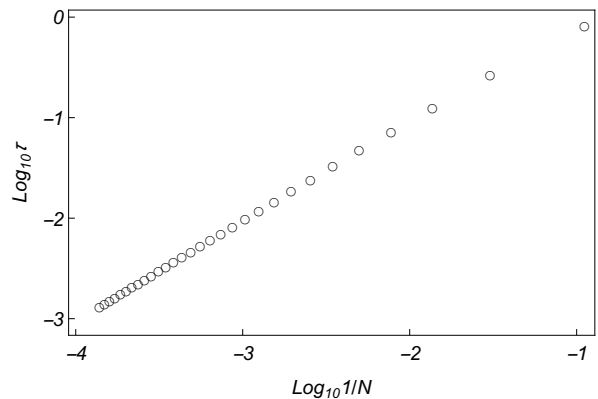


FIG. 7: Behavior of the chirality  $\tau$  for ground states that are eigenvalues of the momentum operator as a function of the length of the chain  $N$ . The data are obtained for the XY chain setting  $\gamma = 0.6$  and  $h = 0.4$

#### IV. FIDELITY

The peculiar behavior of the ground-states in the region  $|h| < h^*$  can be captured by the ground-state fidelity that quantifies how much a system reacts to a small change in the Hamiltonian parameters. Indeed, for a parameters-depending Hamiltonian  $H(\vec{\lambda})$ , the ground-state fidelity is defined as the square modulus of the overlap between two ground-states associated with slightly different sets of parameters, i.e.

$$\mathcal{F}(\vec{\lambda}) = \left| \langle G(\vec{\lambda}) | G(\vec{\lambda} + d\vec{\lambda}) \rangle \right|. \quad (11)$$

As we have already seen, in the region  $|h| < h^*$ , the ground state is no more represented by the vacuum state of the even sector, but by states with 1 or 2 occupied

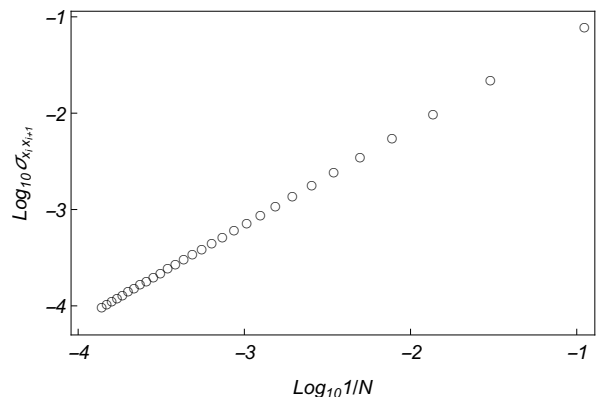


FIG. 8: Variance of the spatial distribution for the two-point spin correlation functions  $\langle \sigma_i^x \sigma_{i+1}^x \rangle$  for ground states obtained as a real symmetric combination of the two ground states with a definite momentum, as a function of the length of the chain  $N$ . The data are obtained for the XY chain setting  $\gamma = 0.6$  and  $h = 0.4$

fermionic levels, depending on the parity sector in which the ground-state manifold falls. In this situation, we have two different possibilities for the ground-state fidelity. The first is that the states  $|G(\vec{\lambda})\rangle$  and  $|G(\vec{\lambda} + d\vec{\lambda})\rangle$  are orthogonal, either because they live in different parity sectors and hence are characterized by a different number of fermions, or because the fermions occupy different fermionic modes.

The second possibility is that both sets of parameters that provide the two ground states are on the same parabola  $h = c(1 - \gamma^2)$ . In this case the ground-state fidelity does not cancel out identically and, depending on the parity, can be written as

$$\mathcal{F} = \prod_{q \in \Gamma_2^+ / \{\bar{q}^+\}} \cos(\bar{\theta}_q - \theta_q), \quad (12)$$

for the even parity and

$$\mathcal{F} = \prod_{q \in \Gamma_2^- / \{\bar{q}^-\}} \cos(\bar{\theta}_q - \theta_q), \quad (13)$$

for the odd one. These expressions are very similar to the ones characterizing the ground-state fidelity of both the unfrustrated systems and the region with  $|h| > h^*$ .

Along these parabolas it is possible to evaluate also the fidelity susceptibility  $\chi$  that, by definition, is equal to the leading order of the expansion of the ground-state fidelity.

$$\mathcal{F} \approx 1 - \frac{1}{2} \chi d\gamma^2, \quad (14)$$

Such a quantity has been widely studied in the context of the unfrustrated XY chain [25, 26], proving to be able to correctly predict the phase transition at  $h = \pm 1$  and  $\gamma = 0$  [30]. In agreement with the Anderson orthogonality catastrophe [9, 10], the fidelity susceptibility always tends to diverge in the thermodynamic limit. However, while in a regular point, this divergence is only extensive, it becomes super-extensive close to a quantum phase transition [26]. Therefore, to study the behavior of the fidelity susceptibility in the thermodynamic limit let us introduce the re-normalized fidelity susceptibility  $\tilde{\chi}$  obtained by dividing  $\chi$  by the system volume. After a long but straightforward evaluation it is possible to prove (see Appendix for details) that, independently from the parity sector, the normalized fidelity susceptibility is

$$\tilde{\chi} = \frac{1}{16} \frac{1 + c^2(1 + \gamma)^3(3\gamma - 1)}{\gamma(1 + \gamma)^2(1 - c^2(1 - \gamma^2)^2)}. \quad (15)$$

One can check, and Fig. 9 confirms, that the re-normalized fidelity susceptibility diverges at  $\gamma \rightarrow 0$ , hence signaling the presence of the critical phase of the quantum XX chain, i.e. the continuous symmetry model emerging by setting  $\gamma = 0$ .

However, as noted above, if we do not assume that  $\vec{\lambda}$  and  $\vec{\lambda} + d\vec{\lambda}$  are on the same parabola, the ground

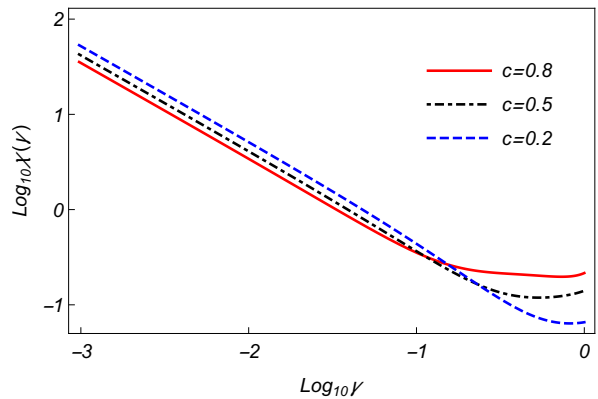


FIG. 9: Thermodynamic limit of the global state fidelity susceptibility  $\tilde{\chi}$  along manifolds of constant momentum  $\tilde{q}$  obtained moving along the parabola  $h = c(1 - \gamma^2)$  as a function of  $\gamma$ . Going towards  $\gamma = 0$  the fidelity susceptibility diverges signaling the presence of the quantum phase transition between the anisotropic XY model and the isotropic XX one.

state fidelity vanishes identically as it occurs within the gapless phases of systems with continuous symmetries. In the latter case, to avoid the problem associated with the scaling analysis of such a ground-state fidelity, it is normal to resort to the reduced fidelity [11, 29, 34, 35]. The reduced fidelity can be seen as a generalization of the ground state fidelity, and it represents the overlap between the reduced density matrices for a fixed subsystem, obtained from ground states corresponding to different parameters, i.e.

$$\mathcal{F}_{RA} = \text{Tr} \sqrt{\rho_A(\vec{\lambda})^{1/2} \rho_A(\vec{\lambda} + d\vec{\lambda}) \rho_A(\vec{\lambda})^{1/2}} \quad (16)$$

Here  $\rho_A(\vec{\lambda})$  ( $\rho_A(\vec{\lambda} + d\vec{\lambda})$ ) denotes the reduced density matrix of the ground state  $|G(\vec{\lambda})\rangle$  ( $|G(\vec{\lambda} + d\vec{\lambda})\rangle$ ), obtained by tracing out all the degrees of freedom associated to sites outside the chosen subset  $A$ . Among all the possibilities we decided to focus on the reduced matrix obtained by projecting the ground state on two nearest-neighbor spins, but other choices lead to similar results. The reduced density matrix on two nearest-neighbor sites can be written in terms of the spin correlation functions [36] as

$$\rho_{ij} = \frac{1}{4} \sum_{\alpha, \beta=0, x, y, z} \langle \sigma_i^\alpha \sigma_j^\beta \rangle \sigma_i^\alpha \otimes \sigma_j^\beta, \quad (17)$$

where  $\sigma^0$  denotes the identity and the analytic expressions for the correlation functions appearing in (17) are presented in the Appendix.

The results obtained for the reduced fidelity, in a system composed of 1001 sites, by keeping the value of  $\gamma$  fixed and changing  $h$  with a uniform step equal to  $10^{-4}$  are shown in Figure 10.

In the chiral region  $h < h^*$  we plot two sets of points: the lowest ones refer to the reduced fidelity while moving along one of the parabolas which keep the occupied



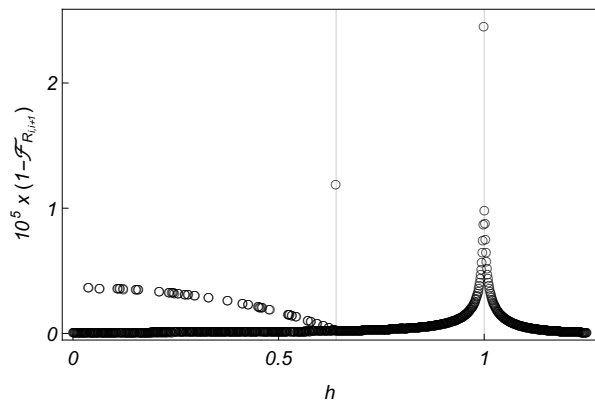


FIG. 10: Reduced fidelity obtained projecting a ground state eigenstate of the momentum operators into the Hilbert space defined by two nearest neighbor spins. The data are obtained considering an XY spin chain made of 1001 spins, fixing  $\gamma = 0.6$  and moving  $h$  from 0 to 1.25. For  $h < h^*$  the lower points refer to movement along a parabola  $h = c(1 - \gamma^2)$ , while the higher values represent a generic flow in which neighboring ground states are characterized by different occupied modes.

modes in the ground state fixed, while the higher ones represent a generic change for which neighboring ground states have vanishing overlaps and even the reduced fidelity gets significantly dampened. Note that a clear discontinuity is observable at the boundary of the chiral region for  $h = h^*$ , where an isolated point develops, which reflects the fact that outside the chiral region the ground state is a vacuum and thus has different correlation functions compared to those for  $h < h^*$ . However, consistently with the analysis made for the energy derivatives near  $h = h^*$ , in Fig. 11 we can observe that the value of this discontinuity decreases proportionally to  $1/N^2$  and therefore disappears in the thermodynamic limit. Similar analysis can be performed for all other points in which the reduced fidelity shows a discontinuity, always yielding a discontinuity that vanishes algebraically with the chain length and hence, in the thermodynamic limit, the behavior of the reduced fidelity for the topologically frustrated spin models is indistinguishable from the one of the unfrustrated models. We should remark, here, that in systems with continuous symmetry, the region of crossovers between different ground states is a true quantum phase and thus the discontinuity at the boundary survives the thermodynamic limit [11].

Clearly, since on one side the whole ground state fidelity is singular and produces a foliation of the phase space, while the two sites reduced fidelity adopts continuity in the thermodynamic limit, a crossover is expected between two behaviors if more sites are included in the subset  $A$ , ideally scaling with the total chain length. However, such analysis cannot be carried out analytically and requires too heavy of a numerical study, which is beyond the scope of the current work.

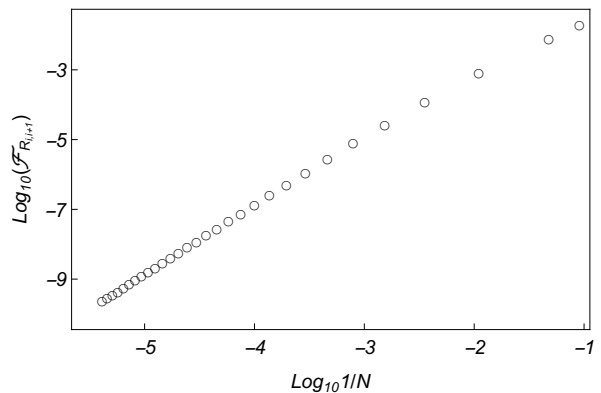


FIG. 11: Reduced fidelity at the line  $h = h^*$  obtained projecting a ground state eigenstate of the momentum operators into the Hilbert space defined by two next neighbor spins as function of the size of the system. The data are obtained considering  $\gamma = 0.6$ . Although at finite sizes a discontinuity is evident, in the thermodynamic limit it vanishes algebraically.

## V. CONCLUSION

In conclusion, we have seen how, in presence of topological frustration, a completely anisotropic Heisenberg chain, which presents only discrete rotational symmetries associated with finite sets of quantum numbers, is characterized by a region of parameter space in which the system mimics that of a system with continuous symmetries. In fact, in analogy with the latter, the system not only presents a gapless energy spectrum with a finite Fermi momentum, but shows, in the thermodynamic limit, a ground-state characterized by a continuous cross-over between two-dimensional mutually orthogonal manifolds. Each one of these manifolds is spanned by eigenstates of the lattice momentum with the same eigenvalues but opposite sign. This fact has several interesting consequences. At first, since these states are characterized by a non-zero momentum, when the system is made of a finite number of spins, they show a non-zero chirality that vanishes in the thermodynamic limit. At the same time, any non-trivial linear combination of such states produces a new ground-state violating the invariance under spatial translation, which, in the case of finite systems, can be observed through the variance associated with the spatial distribution of local observables, but which are zeroed when the dimension of the system diverges. This chiral region is separated from the rest by a threshold line that separates it from a region in which the system is still gapless but the ground state is unique and characterized by a zero moment state. Our analysis clearly shows that such change in the ground state degeneracy is not mirrored in the behavior of the energy. Indeed, in the thermodynamic limit, all energy derivatives are analytical, and hence the transition has to be one akin to a BKT transition. However, the disappearance in the thermodynamic

limit of both properties that characterize this region of parameter space supports the idea that we are looking at a boundary transition whose effects disappear when the size of the system diverges.

Consistently with this picture, the ground state fidelity obtained by continuously varying the parameters of the system, in the thermodynamic limit, is identically zero in almost all directions. The only exception is obtained when the change of the Hamiltonian parameters is carried out in such a way as to keep the momenta characterizing the ground state manifold constant, which, in the particular case of the XY model for which it is possible to carry out an analytical treatment, occurs when the ratio  $h/(1-\gamma^2)$  is kept constant.

However, despite these results, several points concerning this new region of the parameter space of topologically frustrated systems still remain unanswered. For example, it is not yet clear whether it is possible to characterize this new phase from the topological point of view. Most of all, it is important to test the resilience of the described phenomenology to the presence of localized defects, in view of its possible exploitation for quantum technologies. These and other topics will be dealt with in future papers which are already in preparation.

## ACKNOWLEDGMENTS

We thank Vanja Marić for numerous discussions and for preliminary work from which the idea for the this work stemmed. A. G. Catalano acknowledges support from the MOQS ITN programme, a European Union's Horizon 2020 research and innovation programme under the Marie Skłodowska-Curie grant agreement number 955479.. S.M.G and F.F. acknowledges support from the Croatian Science Funds Project No. IP-2019-4-3321 and the QuantiXLie Center of Excellence, a project co-financed by the Croatian Government and European Union through the European Regional Development Fund—the Competitiveness and Cohesion Operational Programme (Grant KK.01.1.1.01.0004).

## Appendix A: Solution of the topologically frustrated XY model

It is well known that the XY model in equation (2) can be diagonalized exactly. The standard procedure prescribes a mapping of spin operators into fermionic ones, which are defined by the Jordan-Wigner transformation:

$$\sigma_j^- = \prod_{l<j} \sigma_l^z \psi_l^\dagger, \quad \sigma_j^+ = \prod_{l<j} \sigma_l^z \psi_j \quad (\text{A1})$$

where  $\psi_l$  ( $\psi_l^\dagger$ ) are fermionic annihilation (creation) operators. In terms of such operators, taking into account

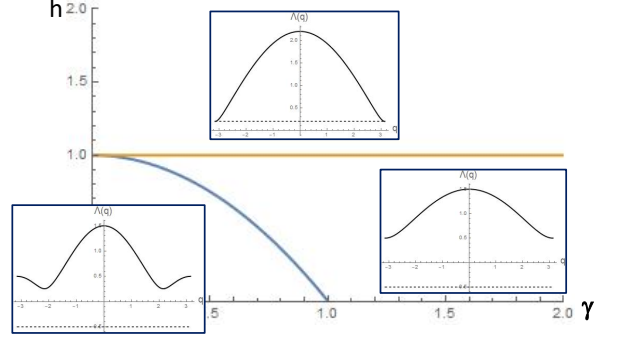


FIG. 12: Phase diagram in the  $(\gamma, h)$  space of the frustrated XY chain: the line at  $h = 1$  is the phase transition separating the frustrated phase from a phase where FBC do not affect the behavior of the system. The parabola  $h = 1 - \gamma^2$  separates the chiral region from the region with a unique ground state. Instances of the single particle dispersion relation eq. (5) are plotted in the various regions together with the energy of the  $\pi$  mode (dashed line), whose occupation lowers the energy of the system for  $h < 1$ .

the periodic boundary conditions and discarding constant terms, the Hamiltonian thus becomes

$$H = \sum_{j=1}^{N-1} \left[ \psi_{j+1}^\dagger \psi_j + \psi_j^\dagger \psi_{j+1} + \gamma (\psi_j^\dagger \psi_{j+1}^\dagger + \psi_{j+1} \psi_j) \right] \quad (\text{A2})$$

$$+ 2h \sum_{j=1}^N \psi_j^\dagger \psi_j + \Pi^z \left[ \psi_1^\dagger \psi_N + \psi_N^\dagger \psi_1 + \gamma (\psi_N^\dagger \psi_1^\dagger + \psi_1 \psi_N) \right].$$

The latter expression is not quadratic itself, but reduces to a quadratic form in each of the parity sectors of  $\Pi^z$ . Therefore, it is convenient to write it in the form

$$H = \frac{1 + \Pi^z}{2} H^+ + \frac{1 - \Pi^z}{2} H^-,$$

where both  $H^\pm$  are quadratic. Hence we can bring the Hamiltonian into a free fermion form by means of two final steps. First, we perform a Fourier transform

$$\psi_q = \frac{e^{-i\pi/4}}{\sqrt{N}} \sum_{j=1}^N e^{-iqj} \psi_j. \quad (\text{A3})$$

It is worth noting that, due to the different quantization conditions,  $H^\pm$  are defined on two different sets of fermionic modes, respectively  $q \in \Gamma^- = \{\frac{2\pi n}{N}\}_{n=0}^{N-1}$  in the odd sector and  $q \in \Gamma^+ = \{\frac{2\pi}{N}(n + \frac{1}{2})\}_{n=0}^{N-1}$  in the even one. Finally a Bogoliubov rotation in Fourier space

$$b_q = \cos \theta_q \psi_q + \sin \theta_q \psi_{-q}^\dagger, \quad (\text{A4})$$

with a momentum-dependent Bogoliubov angles

$$\theta_q = \frac{1}{2} \arctan \left( \frac{\gamma \sin q}{h + \cos q} \right) \quad q \neq 0, \pi, \quad \theta_{0,\pi} = 0. \quad (\text{A5})$$

leads to the Hamiltonians in equations (4a) and (4b). For the sake of simplicity, let us focus on the analysis of the model for values of the local field  $h > 0$ . With this limitation, a key point is to observe that the  $\pi$ -mode is the only one that can be characterized by a negative excitation energy. As depicted in Fig. 12, we can then partition the phase diagram with  $h \geq 0$  and  $0 \leq \gamma \leq 1$  into three regions:

**I**  $h > 1$ : In this case, every excited mode brings a positive energy to the system and hence the lowest energy state is the Bogoliubov vacuum state  $|\emptyset^+\rangle$  falling in the even parity sector. Such a state is separated from the rest of the spectrum by a finite amount of energy equal to the minimum energy carried by the presence of a single Bogoliubov fermion in the system.

**II**  $1 - \gamma^2 \leq h \leq 1$ : In this region, the presence of a fermion in the  $\pi$ -mode, differently from all other modes in the system, is associated with a negative contribution to the total energy. Hence, when populated, the  $\pi$ -mode lowers the energy of the system by a finite amount of energy equal to  $|\epsilon(\pi)|$ . Therefore, it would be energetically favorable to populate this fermionic mode. However, the  $\pi$ -mode exists only in the even parity sector where the addition of a single excitation is forbidden by the parity constraint. Therefore to obtain a physical state in which the  $\pi$ -mode is populated we have to consider a state with two fermions in which the second lives in a different fermionic mode. But the addition of such a second fermion raises the energy by an amount that is greater than  $\epsilon(\pi)$ . For this reason, the lowest energy state of the even sector in this region is still its Bogoliubov vacuum  $|\emptyset^+\rangle$ . In the odd sector, states with a single excitation are allowed, but all fermionic modes hold positive energy and, it is easy to check that each state that can be defined in this sector has an energy greater than the one associated to  $|\emptyset^+\rangle$ . Despite this, the lowest admissible states in this sector, those with one occupied mode with momentum closest to  $\pi$  (exactly  $\pi$  is not possible because of the quantization rule of this sector) have an energy gap closing as  $1/N^2$  compared to  $|\emptyset^+\rangle$ .

Therefore, the ground state of the whole Hamiltonian is still the Bogoliubov vacuum  $|\emptyset^+\rangle$ . However, differently from the previous case, the ground state is no longer separated by a finite energy gap. In fact, due to the form of the dispersion relation, one can easily see that the energy gap closes quadratically in the thermodynamic limit and that there is an alternation between states with different parity.

**III**  $h < h^* = 1 - \gamma^2$ : Here, the dispersion relation (5) develops two symmetric minima at  $q = \pm(\tilde{q})$ , where  $\tilde{q}$  is given by eq. (7). Let us underline that, generally in finite size systems,  $\tilde{q}$  is not an allowed

momentum, i.e.  $\tilde{q} \notin \Gamma^+$  and  $\tilde{q} \notin \Gamma^-$ . Therefore we define two different momenta  $\tilde{q}^+$  and  $\tilde{q}^-$ , that are the elements of  $\Gamma^+$  and  $\Gamma^-$  respectively, that are closer to  $\tilde{q}$  for which the energy associated with the function  $\Lambda(q)$  reaches local minima.

The presence of these local minima is extremely relevant for the ground state of our system. In fact, in the even sector, since now  $\Lambda(\pm k) < \Lambda(\pi)$  the system can fulfill the parity constraint by adding two modes and still keep a total negative energy contribution compared to the vacuum. Therefore, the lowest energy state manifold of the even parity is doubly degenerate, and it is identified by the states  $|g_2^\pm\rangle = b_{\pm\tilde{q}^+}^\dagger b_\pi^\dagger |\emptyset^+\rangle$ . Moreover, in the odd parity sector, we find that the lowest energy state manifold is two-fold degenerate and it is completely described by the states  $b_{\pm\tilde{q}^-}^\dagger |\emptyset^-\rangle$ . The energy of these two manifolds are equal to eqs. (8a,8b). Which is the lesser among these two energies, and therefore which is the two-dimensional manifold that plays the role of the ground-state, depends on the distance of  $\tilde{q}$  from  $\tilde{q}^+$  and  $\tilde{q}^-$ . This leads to repeated crossovers between states belonging to the even sector and states to the odd one. The number of these level crossings increases as the size of the chain tends to the thermodynamic limit.

## Appendix B: Global state fidelity and fidelity susceptibility

In order to evaluate the ground state fidelity in eq. (11), we observe that all ground-states can be written starting from the vacuum states  $|\emptyset^+\rangle$  and  $|\emptyset^-\rangle$ . In terms of the Bogoliubov angles  $\theta_q$ , they can be formulated like

$$|\emptyset^+\rangle = |0_\pi\rangle \bigotimes_{q \in \Gamma_2^+} \left( \cos \theta_q |0\rangle_q |0\rangle_{-q} - \sin \theta_q |1\rangle_q |1\rangle_{-q} \right) \quad (\text{B1a})$$

$$|\emptyset^-\rangle = |0_0\rangle \bigotimes_{q \in \Gamma_2^-} \left( \cos \theta_q |0\rangle_q |0\rangle_{-q} - \sin \theta_q |1\rangle_q |1\rangle_{-q} \right) \quad (\text{B1b})$$

where  $\Gamma_2^+$  ( $\Gamma_2^-$ ) is the subset of momenta  $q \in \Gamma^+$  ( $q \in \Gamma^-$ ) that live in the interval  $q \in (0, \pi)$ . From these expressions it is easy to obtain that, in the region  $h > h^*$  where the ground state coincide with  $|\emptyset^+\rangle$ , the ground-state fidelity, becomes

$$\mathcal{F} = \prod_{q \in \Gamma_2^+} \cos(\theta'_q - \theta_q), \quad (\text{B2})$$

where  $\theta_q$  ( $\theta'_q$ ) are the Bogoliubov angles associated to the set of parameters  $\vec{\lambda} = \{\gamma, h\}$  ( $\vec{\lambda} + d\vec{\lambda} = \{\gamma + d\gamma, h + dh\}$ ).

The situation completely changes entering in the region  $|h| < h^*$ . In this case, the ground state is no more represented by the vacuum state in the even sector, but

by states obtained by populating 1 or 2 fermionic levels, depending on the parity sector in which the ground-state manifold lives. In this situation, we have two different cases. The first is when the two ground states are characterized by having either different numbers of fermions or fermions living in different modes. These occur, in the thermodynamic limit, if the two sets of parameters are not on the same parabola  $h = c(1 - \gamma^2)$  where  $c$  is a constant obeying to the constraint  $|c| \leq 1$ . In this case, the overlap between the two states is reduced to the expectation value of either operators like  $b_q^\dagger b_{q'}$  with  $q \neq q'$ , or of single creation (annihilation) operators on the vacuum states. But, from the expression of the vacuum states in eqs. (B1) it is easy to see that this expectation value is zero, and therefore also the ground-state fidelity vanishes. On the contrary, in the case in which both ground states associated with the two sets of parameters are obtained from the vacuum states by exciting the same fermionic levels, i.e., for large  $N$ , if they are both on the same parabola  $h = c(1 - \gamma^2)$ , the ground-state fidelity does not cancel out identically. Hence, depending on the parity, in the even sector the ground-state fidelity becomes that in eqs. (12,13).

Differently from all the other paths in the region  $|h| < h^*$ , along these parabolas it is possible to evaluate also the fidelity susceptibility that, by definition, is equal to the leading order of the expansion of the ground-state fidelity eq. (14). The susceptibility  $\chi$  is expected to be proportional to the system size in the non critical phase. In the case the ground-states are in the even sector it reads

$$\chi = \sum_{q \in \Gamma^+ / \{\tilde{q}^+\}} \left( \frac{\sin \theta_q (c(1 + \gamma^2) - \cos \theta_q)}{2(\gamma^2 \sin^2 \theta_q + (\cos \theta_q + c(\gamma^2 - 1))^2)} \right)^2 \quad (\text{B3})$$

while in the odd sector the expression of the terms inside the sum is the same with the sum extending to  $q \in \Gamma^- / \{\tilde{q}^-\}$ . By introducing the normalized fidelity susceptibility  $\tilde{\chi} \equiv \chi/N$ , in the thermodynamic limit, we are able to obtain a result independent from the parity sector of the ground-state

$$\tilde{\chi} = \frac{1}{8\pi} \int_0^\pi dx \left[ \frac{\sin x (c(1 + \gamma^2) - \cos x)}{[c(\gamma^2 - 1) + \cos x]^2 + \gamma^2 \sin^2 x} \right]^2 \quad (\text{B4})$$

This integral can be solved analytically using contour integration in the complex plane, upon changing variable to  $z = e^{ix}$  obtaining eq. (15).

### Appendix C: Majorana Correlation functions

By knowing the ground-states in the different regions of parameter space, it is possible to evaluate the spin correlation functions following the approach described in detail in Ref. [37]. It is based on the introduction of the Majorana fermionic operators  $A_i$  and  $B_i$  defined as

$$A_i \equiv \psi_i^\dagger + \psi_i; \quad B_i \equiv \imath (\psi_i - \psi_i^\dagger), \quad (\text{C1})$$

and the use of Wick's theorem [38]. Indeed, each spin correlation function in which we are interested can be mapped, with the help of the Jordan-Wigner transformation in (A1) and the definition in (C1) in a string of Majorana operators on different spins. Then, with the help of Wick's theorem, the expectation value of such a string can be reduced to a Pfaffian in which each single element is the expectation value of a product of two different Majorana operators. Thereby each spin correlation function can be reduced to the evaluation of a particular function of four kind of expectation values i.e.  $\langle A_l A_j \rangle$ ,  $\langle B_l B_j \rangle$ ,  $\langle A_l B_j \rangle$  and  $\langle A_j B_l \rangle = -\langle B_l A_j \rangle$  where  $\langle \cdot \rangle$  stands for the expectation value on a specific ground-state and the indices  $l$  and  $j$  run over all sites of the system.

For  $h > 1$  the ground state of the system has the form of eq. (B1) and it is easy to obtain for the Majorana correlation functions  $\langle B_l A_j \rangle$

$$\langle B_l A_j \rangle = \frac{\imath}{N} \sum_{q \in \Gamma^+} [\sin 2\theta_q \sin(qr) + \cos 2\theta_q \cos(qr)] \quad (\text{C2})$$

where, for brevity, we have defined  $r = j - l$ , while  $\langle A_l A_j \rangle = \langle B_l B_j \rangle = \delta_{l,j}$ . For  $h^* < h < 1$  the ground state of the system still has the form of eq. (B1), but Majorana correlation functions change. In fact, moving from values of the local field greater than 1 to less than 1, we have that while in the first case the energy associated with the momentum  $q = \pi$  was positive, now it turns negative. Hence, while  $\langle A_l A_j \rangle$  and  $\langle B_l B_j \rangle$  remain equal to  $\delta_{l,j}$ , the change in the sign of the energy of the fermionic mode induces a change in the sign of its contribution to the Majorana correlation functions  $\langle A_l B_j \rangle$  that become

$$\begin{aligned} \langle A_l B_j \rangle &= \frac{2\imath(-1)^r}{N} + \frac{\imath}{N} \sum_{q \in \Gamma^+} \sin 2\theta_q \sin(qr) \\ &\quad + \frac{\imath}{N} \sum_{q \in \Gamma^+} \cos 2\theta_q \cos(qr) \end{aligned} \quad (\text{C3})$$

For  $0 \leq h < h^*$  the situation becomes more complex since not only we have a continuous crossover among even and odd states, but also because each single ground-state manifold is two-fold degenerate even for finite  $N$ . Let us consider the two cases, i.e. the manifold living in the even or the odd sector, separately. In the latter case, i.e. if the ground-state manifold falls in the odd-parity sector, all its elements can be written as

$$|g^-\rangle = \left( u b_{\tilde{q}^-}^\dagger + v b_{\tilde{q}^-} \right) |\theta^-\rangle \quad (\text{C4})$$

where  $u$  and  $v$  are complex coefficients obeying the normalization conditions  $|u|^2 + |v|^2 = 1$ . Due to the presence of the fermions in the modes  $\pm \tilde{q}^-$  we obtain that the Majorana correlation functions  $\langle A_l A_j \rangle$  and  $\langle B_l B_j \rangle$  are no more equal to zero when  $l \neq j$ , but become

$$\langle A_l A_j \rangle = \langle B_l B_j \rangle = \delta_{l,j} + \frac{2\imath}{N} (|v|^2 - |u|^2) \sin(r\tilde{q}^-). \quad (\text{C5})$$

Moreover, also the correlation functions  $\langle A_l B_j \rangle$  acquire a state dependent correction and become

$$\begin{aligned} \langle A_l B_j \rangle = & \frac{\imath}{N} \sum_{q \in \Gamma^-} [\sin 2\theta_q \sin(qr) + \cos 2\theta_q \cos(qr)] \\ & - \frac{2\imath}{N} [\sin 2\theta_{\tilde{q}^-} \sin(r\tilde{q}^-) + \cos 2\theta_{\tilde{q}^-} \cos(r\tilde{q}^-)] \\ & + 4|uv^*| \cos(\tilde{q}^-(l+j) + \alpha) \end{aligned} \quad (C6)$$

where  $\alpha$  is the phase of the complex number  $uv^*$ .

On the other hand, in the even sector of the parity the general ground state can be written as

$$|g^+\rangle = b_\pi^\dagger \left( ub_{\tilde{q}^+}^\dagger + vb_{\tilde{q}^+}^\dagger \right) |\emptyset^+\rangle \quad (C7)$$

Similarly to the odd case we recover

$$\langle A_l A_j \rangle = \langle B_l B_j \rangle = \delta_{l,j} + \frac{2\imath}{N} (|v|^2 - |u|^2) \sin(r\tilde{q}^+). \quad (C8)$$

and

$$\begin{aligned} \langle A_l B_j \rangle = & \frac{\imath}{N} \sum_{q \in \Gamma^+} [\sin 2\theta_q \sin(qr) + \cos 2\theta_q \cos(qr)] \\ & - \frac{2\imath}{N} [\sin 2\theta_{\tilde{q}^+} \sin(r\tilde{q}^+) + \cos 2\theta_{\tilde{q}^+} \cos(r\tilde{q}^+)] \\ & + 4|uv^*| \cos(\tilde{q}^+(l+j) + \alpha) \end{aligned} \quad (C9)$$

- 
- [1] D. Jaksch, C. Bruder, J. I. Cirac, C. W. Gardiner, and P. Zoller, "Cold Bosonic Atoms in Optical Lattices", *Physical Review Letters* **81**, 3108 (1998).
- [2] , D. Porras and J. I. Cirac, "Effective Quantum Spin Systems with Trapped Ions", *Physical Review Letters* **92**, 207901 (2004).
- [3] , S. Zippilli, M. Johanning, S. M. Giampaolo, Ch. Wunderlich and F. Illuminati, "Adiabatic quantum simulation with a segmented ion trap: Application to long-distance entanglement in quantum spin systems", *Physical Review A* **89**, 042308 (2014).
- [4] H. Labuhn, D. Barredo, S. Ravets, S. de Léséleuc, T. Macrì, T. Lahaye and A. Browaeys, "Realizing quantum Ising models in tunable two-dimensional arrays of single Rydberg atoms", *Nature* **534**, 667 (2016).
- [5] J. Goldstone, A. Salam and S. Weinberg, "Broken Symmetry", *Physical Review* **127**, 970 (1962)
- [6] W. F. Wreszinski, "Goldstone's theorem for quantum spin systems of finite range", *Journal of Mathematical Physics* **17**, 109 (1976);
- [7] N.D. Mermin, H. Wagner, "Absence of Ferromagnetism or Antiferromagnetism in One- or Two-Dimensional Isotropic Heisenberg Models", *Phys. Rev. Lett.* **17**, 22 (1966).
- [8] F. Franchini, *An introduction to integrable techniques for one-dimensional quantum systems*, Lecture Notes in Physics **940**, Springer (2017).
- [9] P. W. Anderson, "Ground State of a Magnetic Impurity in a Metal", *Physical Review* **164**, 352 (1967).
- [10] P. W. Anderson, "Infrared Catastrophe in Fermi Gases with Local Scattering Potentials", *Physical Review Letters* **18**, 1049 (1967).
- [11] H.-M Kwok, C.-S. Ho, and S.J. Gu, "Partial-state fidelity and quantum phase transitions induced by continuous level crossing", *Physical review A* **78**, 062302 (2008)
- [12] V. Marić, S. M. Giampaolo and F. Franchini, "Quantum phase transition induced by topological frustration", *Communications Physics* **3**, 220 (2020)
- [13] G. Toulouse, "Theory of the frustration effect in spin glasses: I", *Communications on Physics* **2**, 115 (1977).
- [14] J. Vannimenus and G. Toulouse, "Theory of the frustration effect: II. Ising spins on a square lattice", *Journal of Physics C: Solid State Physics* **10**, L537 (1977).
- [15] J.-F. Sadoc and R. Mosseri, "Geometrical Frustration", Cambridge University Press (Cambridge) (1999).
- [16] M. M. Wolf, F. Verstraete and J. I. Cirac, "Entanglement and Frustration in Ordered Systems", *International Journal of Quantum Information* **1**, 465 (2003).
- [17] S. M. Giampaolo, G. Gualdi, A. Monras and F. Illuminati, "Characterizing and Quantifying Frustration in Quantum Many-Body Systems", *Physical Review Letters* **107**, 260602 (2011).
- [18] H. T. Diep, "Frustrated Spin Systems", World Scientific (Singapore) (2013).
- [19] U. Marzolino, S. M. Giampaolo and F. Illuminati, "Frustration, entanglement, and correlations in quantum many-body systems", *Physical Review A* **88**, 020301 (2013).
- [20] C. R. Laumann, R. Moessner, A. Scardicchio and S. L. Sondhi, "Quantum Adiabatic Algorithm and Scaling of Gaps at First-Order Quantum Phase Transitions", *Physical Review Letters* **109**, 030502 (2012).
- [21] S. M. Giampaolo, F. B. Ramos and F. Franchini, "The Frustration of being Odd: Universal Area Law violation in local systems", *Journal of Physics Communications* **3**, 081001 (2019).
- [22] J.-J. Dong, P. Li and Q.-H. Chen, "The a-cycle problem for transverse Ising ring", *Journal of Statistical Mechanics: Theory and Experiment* **2016**, 113102 (2016)
- [23] V. Marić, S. M. Giampaolo and F. Franchini, "The frustration of being odd: how boundary conditions can destroy local order", *New Journal of Physics*, **22**, 083024 (2020)
- [24] P. Zanardi and N. Paunković, "Ground state overlap and quantum phase transitions", *Physical Review E* **74**, 031123 (2006)
- [25] P. Zanardi, M. Cozzini and P. Giorda, "Ground state fidelity and quantum phase transitions in free Fermi systems", *Journal of Statistical Mechanics: Theory and Experiment*, **2007**, L02002 (2007)
- [26] L. Campos Venuti and P. Zanardi, "Quantum Critical Scaling of the Geometric Tensors", *Physical Review Letters* **99**, 095701 (2007).
- [27] P. Zanardi, P. Giorda, and M. Cozzini, "Information-Theoretic Differential Geometry of Quantum Phase Transitions", *Physical Review Letters* **99**, 100603 (2007).
- [28] J.M. Kosterlitz and D.J. Thouless, "Ordering, metastability and phase transitions in two-dimensional systems",

- Journal of Physics C: Solid State Physics **6**, 1181 (1973)
- V.L. Berezinskii, "Destruction of long-range order in one-dimensional and two-dimensional systems having a continuous symmetry group I. Classical systems", *Sov. Phys. JETP* **32**, 493 (1971)
- V.L. Berezinskii, "Destruction of long-range order in one-dimensional and two-dimensional systems having a continuous symmetry group II. Quantum systems", *Sov. Phys. JETP*, **34**, 610 (1972)
- [29] W.-L. You and W.-L. Lu, "Scaling of reduced fidelity susceptibility in the one-dimensional transverse-field XY model", *Physics Letters A* **373**, 1444 (2009)
- [30] M. Kolodrubetz, V. Gritsev, and A. Polkovnikov, "Classifying and measuring geometry of a quantum ground state manifold", *Physical Review B* **88**, 064304 (2013)
- [31] U. Bhattacharya, S. Dasgupta, and A. Dutta, "Exploring chaos in the Dicke model using ground-state fidelity and Loschmidt echo", *Physical review E* **90**, 022920 (2014)
- [32] X. G. Wen, F. Wilczek and A. Zee, "Chiral spin states and superconductivity", *Physical Review B* **39**, 11413 (1989).
- [33] V. Subrahmanyam, "Chirality operators for Heisenberg spin systems", *Physical Review B* **50**, 6468 (1994).
- [34] S.-J. Gu, "Fidelity approach to quantum phase transitions", *International Journal of Modern Physics B* **24**, 4371 (2010).
- [35] J. Ma, L. Xu and H.-N. Xiong, "Reduced fidelity susceptibility and its finite-size scaling behaviors in the Lipkin-Meshkov-Glick model", *Physical Review E* **78**, 051126 (2008).
- [36] T. J. Osborne and M. A. Nielsen, "Entanglement in a simple quantum phase transition", *Physical Review A* **66**, 032110 (2002).
- [37] E. Barouch and B. M. McCoy, "Statistical Mechanics of the XY Model. II. Spin-Correlation Functions", *Physical Review A* **3**, 786 (1971).
- [38] G. C. Wick, "The Evaluation of the Collision Matrix", *Physical Review* **80** 268 (1950).